

# High-speed deformation of copper samples with the use of magnetic pulse method

*Sergey Krivosheev*<sup>1,\*</sup>, *Sergey Magazinov*, and *Dmitrii Alekseev*

<sup>1</sup>Peter the Great Saint-Petersburg Polytechnic University, 195251 Saint-Petersburg, Russia

**Abstract.** The possibility of using the magnetic pulse method for studying the high-speed deformation modes of metals with strain rates up to 100,000 1/s without a preliminary phase of material compression under loading in the microsecond range of durations is shown. 3D calculation of the magnetic field and deformation modes has shown the possibility of creating loading schemes that are free of induced currents in the sample in the zone of maximum mechanical stresses. The first experiments show the need for verification of the Jones-Cook model at high deformation rates.

## 1 Introduction

Magnetic pulse method for creating controlled pressure pulses of microsecond duration in the study of the pulse strength of brittle non-conductive materials revealed a number of common patterns of fracture process [1, 2]. Using of thermodynamic approach for analysis of the results of brittle non-conductive materials fracture process allowed to reveal specific relations among extreme destructive loading, the duration of this loading and specific material parameter – energy storage time [3]. This approach can be used to describe transitions between different states of the loaded system, not only the catastrophic transition caused by fracture, but also elastic-plastic transition associated with a change in shape or deformation under any strain rates. The special feature of this method is the ability to form stressed states in which there is no pre-stressed modes in material, typical for spall test schemes. Implementation of this feature is especially important for the test of metals, composite and laminate materials, with an explicit spatial anisotropy of the deformation characteristics.

## 2 Conductive samples with defect of type of crack

Typical magnetic pulse loading of samples with macro defects is shown in Fig. 1. Selection of parameters of the generator and the magnetic system for generating controlled pressure pulses of microsecond duration can be implemented on the recommendation of [4, 5].

The cross-section of magnetic pulse driver (MPD) busbars was selected with taking into account the integral of the action, at which the material of busbars remains in the solid

---

\* Corresponding author: [ksi.mgd@gmail.com](mailto:ksi.mgd@gmail.com)

phase [6]. An insulating layer of fiberglass with a thickness of 0.1 mm was located between MPD and grooves to exclude the current flow through the sample. The breakdown electric strength of fiberglass is 25 – 30 kV/mm and provides electrical isolation of the MPD from the sample. Such parameters of the insulating layer ensure that a pressure corresponding to the magnetic pressure generated by the MPD is transmitted to the sample.

The tensile strength of fiberglass is approximately 500 MPa and significantly exceeds the elastic limit of the research material. To exclude the impact of possible deformation of the busbars MPD on the parameters passed in the pressure pulse the edges of the busbars are fixed by fiberglass clamps. In this case, the parameters of the magnetic pressure are determined only by the geometry of the MPD and the current flowing through its busbars.

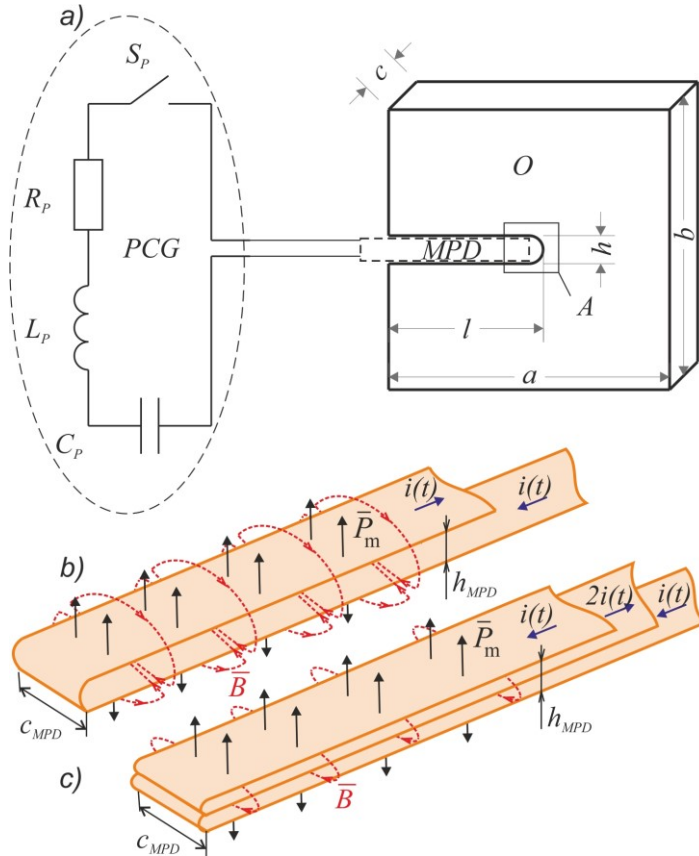


**Fig. 1.** Magnetic pulse loading setup. a) Schematic circuit of pulse current generator (PCG) device and scheme of loading for pulse testing.  $C_p$ ,  $L_p$  - capacity and self-inductance of PCG;  $S_p$  – high-voltage commutation switch;  $R_p$  - resistor;  $O$  – sample under test;  $a$ ,  $b$ ,  $c$  – length, height and thickness of sample;  $h$  and  $l$  – height and length of groove. b) simple MPD; c) quasi-coaxial MPD;  $h_{MPD}$ ,  $c_{MPD}$  - height and thickness of MPD;  $\vec{P}_m$  – vector of magnetic pressure;  $\vec{B}$  – vector of magnetic induction;  $i(t)$  – electric current.

The pressure amplitude can reach 2 - 10 GPa. Such pressure amplitude is sufficient for testing metallic materials. However, the transition to tests of conductive samples imposes a number of limitations related to the possible impact of induced current in the sample on the deformation curves of metal.

### 2.1 Induced currents structure

The simulation results of induced currents structure in metallic sample for the simple magnetic pulse driver (MPD) in the form of a system of flat bars (Fig. 1b) - simple MPD and the quasi-coaxial MPD (Fig. 1c), which are represented in [3], are shown in Fig. 2.

The calculation was performed in a 3D setting with the consideration of the induced currents impact on the sample and the MPD. The used material for the sample and the MPD was copper. Pulsed electrical current in MPD, with duration of 5  $\mu$ s and amplitude of the current 40 kA, was set as the external impact.

Such impulse duration did not cause significant heating of the MPD busbars. The cross section of the MPD busbars was 2×0.2 mm.

Geometric dimensions, in accordance with the designations of Fig.1 were:  $a = b = 3$  cm,  $c = c_{MPD} = 2$  mm,  $l = 1.5$  cm,  $h = 2$  mm,  $h_{MPD} = 1.6$  mm.

The numerical simulation results showed that the use of a simple MPD induced current density in the sample can reach values up to 40 kA/mm<sup>2</sup> or more in the zone of maximum mechanical stress (top of the groove – point M, position 1 in Fig. 2), and the sample heating due to a current flow is approximately 5°C. Calculated magnetic field between simple MPD busbars is 14 T.

According to the data, submitted in [7, 8] it is known that such current density causes the electroplastic effect (EPE), which can influence on the process of deformation. This effect is experimentally observed for low deformation rates and is revealed in the reduction of the yield stress. This reduction of the yield stress may reach 30-40 % for different metals [9]. A negligible amount of experimental data on the impact of EPE on the process of high-speed deformation, e.g. [10], does not exclude the possibility of its manifestation in pulsed load mode.

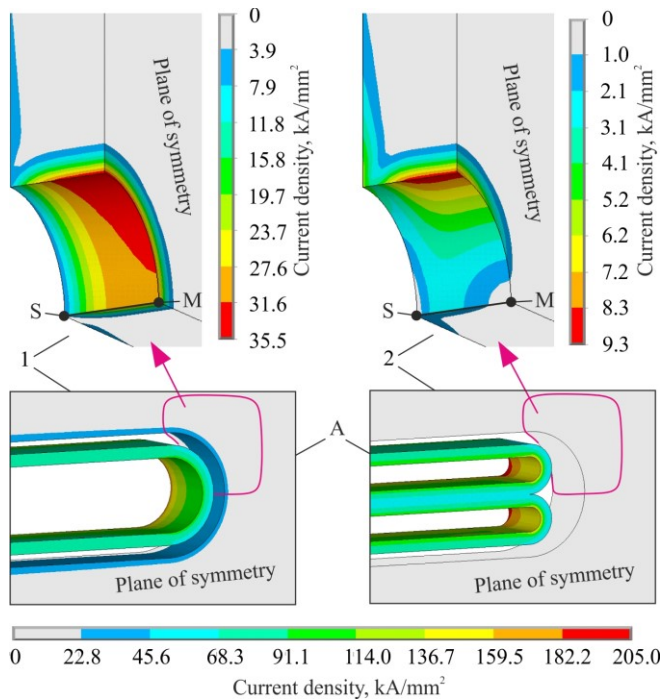


**Fig. 2.** Current density distribution near the groove top for different magnetic pulse drivers at the moment of maximum induced current. SM - line of symmetry

On the contrary, using of the quasi-coaxial MPD (position 2 in Fig. 2) leads to a significant current density reduction and changes the spatial distribution of current density. The quasi-coaxial driver provides the formation of such stressed state in which the local minimum of current density close to zero is in the apex of the groove in point M, thus we can say that in the apex of the groove the zone free from the EPE impact is formed. Calculated magnetic field between quasi-coaxial MPD busbars is 20 T.

The derivation and comparison of the relation between sample deformation and applied magnetic pressure for samples with the use of simple and quasi-coaxial MPD in the same mechanical stress conditions, from the point of view of formation of these fields, will allow to determine the EPE impact on the deformation under pulse loading.

## 2.2 Simulation of Elastic-Plastic deformation

The simulation of elastic–plastic deformation of a copper busbar with macro defect of type of crack in the three-dimension setting was carried out using the ANSYS Autodyn environment [11]. The Johnson–Cook (JC) plasticity model for OFHC copper [12] was selected as a calculation model of deformation. The reliability of mentioned model for various metals is supported by its implementation in different programming environments, e.g. [11]. According to JC model the elastic limit of material varies depending on plastic strain, strain rate  $v_p$ , which must be equal or more then 1/sec, and temperature is described by the next expression:

$$\sigma = [A + B\varepsilon_p^n][1 + C \ln v_p^*][1 - T^{*m}] \quad (1)$$

where  $\varepsilon_p$  is an effective plastic strain,  $v_p^* = v_p/v_p\theta$  is a standardized effective plastic strain rate ( $v_p\theta = 1$  1/s – effective plastic strain rate used for determination parameters of model –  $A$ ,  $B$ , and  $n$ ),  $T^{*m} = (T - T_{room})/(T_{melt} - T_{room})$  is homologous temperature,  $A = 90$  MPa,  $B = 292$  MPa,  $n = 0.31$ ,  $C = 0.025$ ,  $m = 1.09$ ,  $T_{melt} = 1082.9$  °C are model parameters.

The JC fracture model is applied as the failure criterion:

$$D = \sum \Delta\varepsilon / \varepsilon_f^D \quad (2)$$

$$\varepsilon_f^D = [D_1 + D_2 e^{D_3 \sigma^*}][1 + D_4 \ln v_p^*][1 + D_5 T^{*m}] \quad (3)$$

where  $\varepsilon_f$  is an effective fracture strain,  $\Delta\varepsilon$  is the increment of equivalent plastic strain which occurs during an integration cycle,  $\sigma^* = \sigma_m / \sigma_{av}$  is the dimensionless pressure-stress ratio ( $\sigma_{av}$  is the average of the three normal stresses and  $\sigma_m$  is the von Mises equivalent stress).  $T^{*m}$  and  $v_p^*$  are identical to those used in the equation (1).  $D_1 = 0.54$ ,  $D_2 = 4.89$ ,  $D_3 = -3.03$ ,  $D_4 = 0.014$ ,  $D_5 = 1.12$  are parameters of fracture model. When the parameter  $D$  reaches the value 1, the material is destroyed.

The JC plasticity model describes deformation process up to fracture, and the validity of the use of the JC plasticity model is justified by the good correspondence between calculated and experimental deformation curves for different plastically deformable materials at strain rates up to  $\sim 2000$  1/s. For instance, the applicability of JC model for description of the high-speed deformation process for steel 09G2S at strain rates up to 1500 1/s is shown in [13].

The deviation the deformation curve from a linear one due to plastic flow leads to a significant reduction in the achievable stress for the case of the wave loading (curves 1, 2, 3 in Fig. 3a). This leads to the failure to ensure a high strain rate, as it shown in Fig. 3.

Transition to a quasi- stationary mode allows to extend significantly the range of variation of achievable stress, and to provide a large deformation of the material at the top of the groove, until the fracture of the sample (Fig. 3, curve 4.).

The character of the stress state is defined by the characteristic size of the sample  $b$  (Fig. 1) and the loading wavelength  $\lambda = c_l \cdot T$ , where  $c_l$  - speed of sound in the material. If  $\lambda$  is much smaller than  $b$  wave mode is implemented, otherwise, the quasi-static is. Calculations were provided for two samples with different sizes: 1 -  $a = 3$  cm,  $b = 3$  cm,  $c = 1$  mm,  $h = 2$  mm,  $l = 1.5$  cm; 2 -  $a = 12$  cm,  $b = 12$  cm,  $c = 1$  mm,  $h = 2$  mm,  $l = 6$  cm (designations according to Fig. 1).

The quasi-static mode of loading was implemented in the first sample by impacting distributed pulse of pressure with duration  $T = 50 \mu\text{s}$  to groove shores. Wave mode was implemented in the second sample by the impact of the distributed pulse of pressure with duration  $T = 8 \mu\text{s}$ . The results of simulation show that in both cases the maximum stresses are formed in a zone located near the top of the groove (along line MS Fig. 2).

The analysis of numerical simulation results show that when the sample is impacted with an evenly distributed along the shores of the groove pressure created by magnetic pulse driver, it is possible to provide the deformation of the sample at a strain rate of up to  $10^5$  1/s.

The simulation was carried out at the supercomputer centre "Polytechnic" with heterogeneous cluster HPC Tornado. The parameters of one node of the cluster: RSC Tornado - 2 CPU with 14 cores (2xXeon E5-2697v3 2.6 GHz 64 GB RAM).

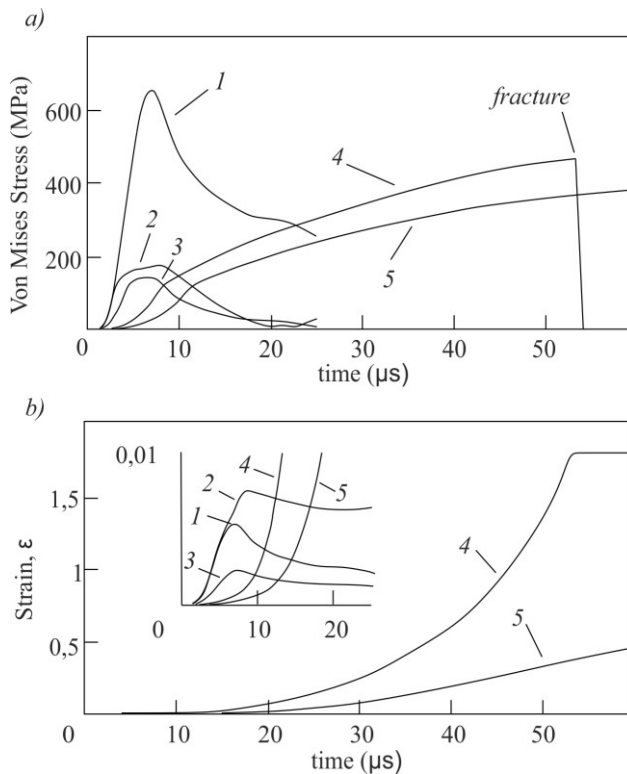


**Fig. 3.** a) Relation between stress on the groove top and time; b) Relation between relative deformation on the groove top and time.

1 -  $P_m = 250$  MPa,  $T = 8 \mu\text{s}$  (excluding plastic deformation); 2 -  $P_m = 250$  MPa,  $T = 8 \mu\text{s}$ ,  $v_p = 1600$  1/s; 3 -  $P_m = 85$  MPa,  $T = 8 \mu\text{s}$ ,  $v_p = 500$  1/s; 4 -  $P_m = 250$  MPa,  $T = 50 \mu\text{s}$ ,  $v_p = 90000$  1/s; 5 -  $P_m = 85$  MPa,  $T = 50 \mu\text{s}$ ,  $v_p = 14000$  1/s.

### 2.3 Experimental setup and procedure

The experimental setup - the pulse current generator GIT-50/12 (storage capacity  $C_p = 12 \mu\text{F}$ , charging voltage  $U_p = 50 \text{ kV}$ , self-inductance  $L_p = 53 \text{ nH}$ ) was used to provide initial test of samples according to the scheme shown in Fig. 1. The material of the sample was copper Cu ETP, sample sizes was  $a = 30 \text{ mm}$ ,  $b = 30 \text{ mm}$ ,  $c = 2 \text{ mm}$ ,  $h = 2 \text{ mm}$ ,  $l = 15 \text{ mm}$ . The hole with diameter  $d_h = 10 \text{ mm}$  (see Fig. 4a) was made in the sample to increase the level of plastic deformation due to the localization of the mechanical stress in the zone between the groove and hole, which leads to a significant increase in stress compared to the sample without a hole.

After charging the generator up to 30 kV, GIT – 50/12 forms pulse current with amplitude  $\sim 360 \text{ kA}$  in a simple magnetic pulse driver. Discharge current was measured by Rogowski coil and has a form of strongly damped sinusoid with the attitude of neighbouring amplitudes  $\sim 0.6$  and period of  $5 \mu\text{s}$ . The corresponding to this current pressure pulse had an amplitude  $\sim 0.7 \text{ GPa}$  in test with magnetic pulse driver with width  $C_{MPD} = 11 \text{ mm}$ . The current lead busbars were fixed with dielectric gasket made of fiberglass to exclude any movement.

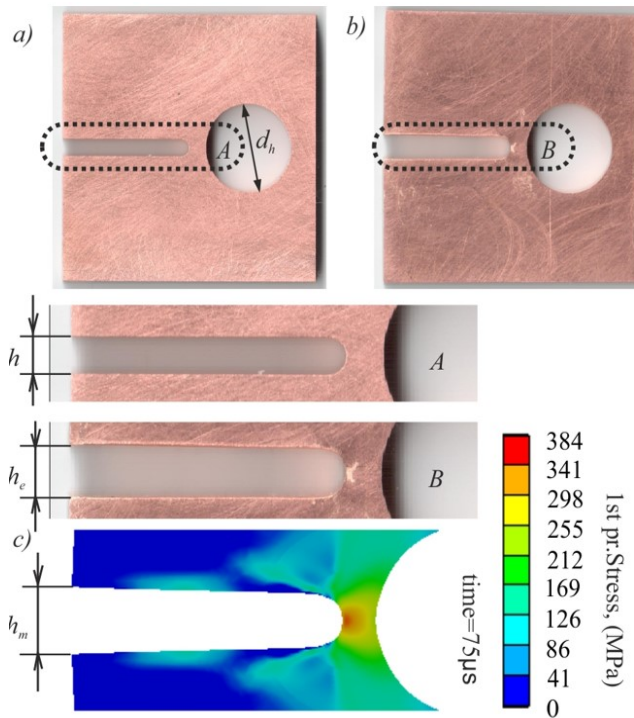


**Fig. 4.** Comparison of experimental data and numerical simulation. a) The sample before testing; b) The sample after testing; c) Numerical Simulation results – 1st principal stress (time = 75  $\mu\text{s}$ ).  $h$ ,  $h_e$ ,  $h_m$  – height of groove before testing, after testing and from simulation;  $d_h$  – hole diameter.

Comparison of experimentally registered permanent deformation with the results of numerical simulation is given in Fig. 4 and shows the inflated value of the groove deformation  $h_m = 3.6 \text{ mm}$ , compared with the experimental value  $h_e = 2.8 \text{ mm}$ . The mismatch of the calculated strain may be due to a variety of factors, including overestimated applied pressure, due to inaccurate recalculation of the current pulse into the magnetic pressure. According to the results of numerical simulation the highest

mechanical stresses during deformation are concentrated in the top of the groove and plastic deformation strain rate reaches  $v_p \sim 15000$  1/s, however the JC model described in paragraph II.B may be insufficiently adequate for a given strain rate

### 3 Conclusion

Analysis of simulation results showed the possibility of using magnetic-pulse method of deformation of conductive materials at strain rates up to  $\sim 100\,000$  1/s. The proposed loading scheme allows to combine the process of deformation with a pulse current exposure and investigating the impact of the electroplastic effect. In addition, transition to higher strain rates will provide data for Johnson – Cook model verification in a wider range of influences.

### References

1. S.I. Krivosheev, N.F. Morozov, Y.V. Petrov, and G.A. Shneerson, *J. Mater. Sci.* **32**, 3, 286-295 (1996)
2. S.I. Krivosheev and G.A. Shneerson, *MEGAGAUSS* (2008).
3. S.I. Krivosheev, N.V. Korovkin, V.K. Slastenko, and S.G. Magazinov, *Int. J. Appl. Mech.* **9**, 293 (2015)
4. S.I. Krivosheev, *Tech. Physics* **50**, 3, 334 (2005)
5. G.A. Shneerson, M.I. Dolotenko, S.I. Krivosheev, *Strong and superstrong pulsed magnetic fields generation* (Walter De Gruyter Incorp., **439**, 2014)
6. Heinz Knoepfel, *Pulsed high magnetic fields: physical effects and generation methods concerning pulsed fields up to the megaoersted level. North-Holland publishing company* (Amsterdam – London , 1970)
7. O.A. Troitskii, and L.G. Maistrenko, *Soviet Mater. Sci.* **8**, 6, 686 (1974)
8. H. Conrad, *Mater. Sci. and Engineer.* **A322**, 100-107 (2002)
9. A.F.Sprecher, S.I. Mannan, H. Conrad, *Acta metal.* **34**, 7, 1145 (1986)
10. B. Kinsey, G. Cullen, A. Jordan, S. Mates, *CIRP Annals – Manufacturing Technology* **62** (2013)
11. ANSYS Academic Research Customer #00420725 (from 2010), Comp Mech Lab
12. G.R. Johnson and W.H. Cook, *J. Eng. Frac. Mech.* **21**, 1, 31 (1985).
13. Vl. Vas. Balandin, Vl. Vl. Balandin, A. M. Bragov, L. A. Igumnov, A. Yu. Konstantinov, and A. K. Lomunov, *Mech. solids* **49**, 6, 666 (2014)